



Transparent, flexible supercapacitors from nano-engineered carbon films

Hyun Young Jung¹, Majid B. Karimi¹, Myung Gwan Hahm^{2,3}, Pulickel M. Ajayan² & Yung Joon Jung¹

SUBJECT AREAS:
MATERIALS SCIENCE
PHYSICS
APPLIED PHYSICS
ELECTROCHEMISTRY

¹Department of Mechanical and Industrial Engineering, Northeastern University, Boston, MA 02115, USA, ²Department of Mechanical Engineering and Materials Science, Rice University, Houston, Texas 77005, USA, ³Research Center for Exotic Nanocarbons, Shinshu University, 4-17-1 Wakasato, Nagano-shi, Nagano 380-8553, Japan.

Received
30 July 2012

Accepted
1 October 2012

Published
26 October 2012

Correspondence and requests for materials should be addressed to Y.J.J. (jungy@coe.neu.edu) or P.M.A. (ajayan@rice.edu)

Here we construct mechanically flexible and optically transparent thin film solid state supercapacitors by assembling nano-engineered carbon electrodes, prepared in porous templates, with morphology of interconnected arrays of complex shapes and porosity. The highly textured graphitic films act as electrode and current collector and integrated with solid polymer electrolyte, function as thin film supercapacitors. The nanostructured electrode morphology and the conformal electrolyte packaging provide enough energy and power density for the devices in addition to excellent mechanical flexibility and optical transparency, making it a unique design in various power delivery applications.

Recently there has been significant interest in using carbon based nanomaterials as supercapacitor electrodes due to several advantages of carbon such as light weight, high electrical conductivity and electrochemical surface area^{1–20}. There is a large number of interesting possibilities in creating new designs for such energy storage devices if the carbon electrodes can be tailored and engineered to fit new functionalities. Here, we demonstrate the design and fabrication of flexible and transparent supercapacitors using a highly structured carbon thin film, structured inside porous templates by chemical vapor deposition. These carbon films consist of arrays of periodic and interconnected nano-cup morphologies of few layer graphitic structure (from now, termed as carbon nanocups - CNC) and are used as thin film electrodes for the supercapacitor devices. CNCs are architectures precisely engineered from graphitic carbon, within porous templates, having up to 10^5 times smaller length/diameter (L/D) ratios compared to conventional nanotubes, and have unique nanoscale cup morphology. Our CNC film-polymer electrolyte composites have three remarkable features for the use as a solid state, thin-film supercapacitor device. First, a CNC film has the high surface area offered by arrays of controlled nanoscale cup structures and highly disordered graphitic layers that are keys for the effective permeation of the polymer electrolyte in supercapacitors. Second, unique nanoscale structural and morphological features of CNC films enable the easy access and faster transport of ions at the electrode/electrolyte interface resulting in higher power capability. Finally, high current carrying capability, substantial mechanical strength, and small effective electrode thickness (10 nm) allow us to build multifunctional (optically transparent and mechanically flexible) reliable thin-film energy storage devices.

Results

Fabrications of nano-engineered carbon films. Fig. 1a and 1b–c shows the scanning electron microscopy (SEM) images of top (concave) and bottom (convex) parts of as-synthesized CNC films (with channels of 80 ± 10 nm in diameter and 140 ± 10 nm in length). By connecting the highly dense and ordered arrays of nanocups with continuous graphitic layer that, large area porous nanostructured films ideal for energy storage electrodes is achieved. To further increase the surface area of CNC films, multi-branched nanocup architecture, with large number of short nanotubes (25 nm in diameter and 330 ± 10 nm in length) grown and attached to the bottom of the CNC films, are fabricated by using multistep anodization process followed by a chemical vapor deposition (CVD) method²¹ (Fig. 1d–f). Through the control of nanopore dimension in anodic aluminum oxide (AAO) templates and CVD conditions, we can precisely tailor the geometry and structure of the nanocup such as length, diameter, L/D aspect ratio, and their wall thickness, which are important factors to determine capacitor behavior, mechanical stability, and optical property of devices. Our calculation reveals that a branched convex CNC films possess 2.3 times higher surface area exposed to the electrolyte than that of a normal convex CNC film (see the method section for the surface area calculation). The length of branched carbon nanotubes is optimized to obtain optical transparency as well as maximized electrochemically active interface between electrodes and polymer electrolyte. Also it is noted that the innermost layer of the concave nanocup (Fig. 1a) has relatively well-ordered

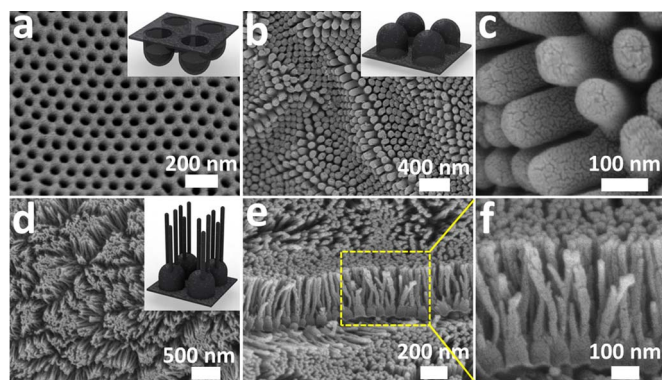


Figure 1 | SEM images of CNCs. SEM images of (a) concave and (b, c) convex and (d–f) branched nanocup films. (c) is high magnification SEM image of (b) convex nanocup with 80 ± 10 nm in diameter and 140 ± 10 nm in length. (e, f) is cross-sectional view of (d) branched nanocup film and (f) is high magnification image of (e), where short carbon nanotubes (25 nm in diameter and 330 ± 10 nm in length) are branched from the bottom of a nanocup. Note that the thickness of CNCs film can be controlled by changing carbon deposition time or carbon concentration during a CVD process. The inset figures show schematics of concave, convex and branched convex nanocup film.

graphitic structure, while the outermost layer which is the surface of the convex part (Fig. 1b–f), is very defective²². When used as a supercapacitor electrode, these defects can act as reactive sites providing an effective charge transfer and good electrode-electrolyte interfaces that minimize the internal resistance of supercapacitor devices. Measured surface electrical conductivity of the CNC film is 117 S/m, which is higher than typical activated carbon electrodes (~ 30 S/m)²³ for supercapacitors.

Fabrications of transparent and flexible supercapacitor devices.

We have fabricated a flexible and transparent thin-film supercapacitor device by impregnating highly porous CNC electrodes (anode and cathode) in transparent polymer electrolyte films. Fig. 2 shows

schematics of the fabrication process of branched CNC-polymer electrolyte thin films and optical images of supercapacitor devices. As shown in the schematics of Fig. 2a, the nanocup films are transferred to polydimethylsiloxane (PDMS) and released by dissolving AAO templates in copper chloride and hydrochloric acid mixture solution to produce transparent and flexible graphitic carbon electrodes. The CNC films are then utilized as a dual function layers in supercapacitor devices where an inner graphitic layer exposed to the electrolyte acts as active electrodes and outer graphitic layer works as current collectors. The fact that ultra-thin and organized arrays of nanostructured graphitic film can be used for both electrodes and current collectors enables us to design and create mechanically flexible and optically transparent supercapacitor film in a scalable and simple manner. For the ionic electrolyte/separator, the polyvinyl alcohol-phosphoric acid (PVA- H_3PO_4) gel electrolyte is then sandwiched between two separated CNC electrode films. For this, PVA- H_3PO_4 polymer solution is poured over the CNC film and spin-coated with 500 rpm to obtain the effective electrolyte thickness (12 μm). CNC films are transparent with transmittance of 71% at 550 nm wavelength (supplemental Fig. S1) and so the fabricated solid state thin film CNC supercapacitor devices are optically transparent (Fig. 2b) and mechanically flexible (Fig. 2c).

Characterizations of the supercapacitors. Cyclic voltammetry (CV) is performed to evaluate the capacitance of all three different types of CNC (concave, convex, and branched convex) electrode based solid state supercapacitors. All CV curves show a very rapid current response on the voltage reversal at each end potential and straight rectangular shapes representing a very small equivalent series resistance of electrodes and faster ionic diffusion in the electrolyte film. The CV curves of CNC devices are measured with various scan rates in the ranges of 10 – 500 mVs^{-1} . Especially when a branched CNC electrode (branched convex) is used (Fig. 3a), nearly rectangular shaped CV curves are obtained even at very high scan rates demonstrating high performance capacitor devices (for concave and convex CNC devices, see supplemental Fig. S2a and S2d). Galvanostatic charge/discharge (CD) is also conducted to evaluate the normalized capacitance and internal resistance of the branched

Figure 2 | Schematics of the fabrication process of a branched CNC based supercapacitor and its optical images. (a) First the CNC films are transferred to PDMS and released by dissolving AAO templates. Then the gel-electrolyte (as electrolyte-separator) is sandwiched between two CNC electrodes (as electrode-current collector) with 12 μm thickness and solidifies after evaporation of water. Optical pictures demonstrating (b) transparent and (c) flexible natures of CNCs supercapacitor devices.

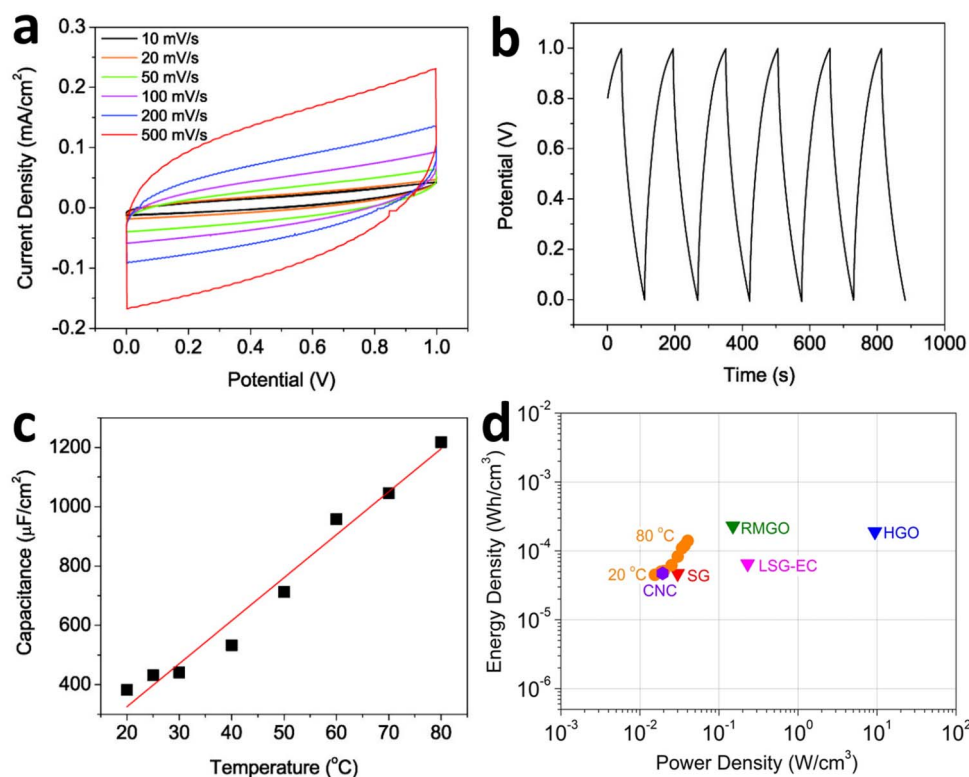


Figure 3 | Electrochemical properties of branched CNC supercapacitor devices. (a) Cyclic voltammetry (CV) measured with 10–500 mVs⁻¹ scan rates. (b) Galvanostatic charge/discharge (CD) results measured at a constant current density of 5 μAcm⁻². The capacitances by the geometrical area calculated from CD curves are 409 μFcm⁻². (c) The capacitance change as a function of temperature (20 °C to 80 °C). (d) CNC devices are compared with various energy storing devices by the Ragone plot that is the values of energy density for power density. (SG: single layer graphene¹⁸, RMGO: reduced multilayer graphene oxide¹⁸, HGO: hydrated graphitic oxide¹⁹, LSG-EC: laser-scribed graphene electrochemical capacitor²⁰).

convex CNC supercapacitor device (for concave and convex CNC devices, see supplemental Fig. S2b and S2e). The E-t responses of the charge process show a triangular shape and mirror image with corresponding discharge counterparts confirming the formation of an efficient capacitor and excellent charge propagation across two electrodes.

The capacitances by the geometrical area calculated from CD curves are 78, 132, 409 μF cm⁻² for concave, convex, and branched CNC supercapacitors, respectively (see method section for the capacitance calculation). Note that we have chosen to use the areal capacitances, and not the gravimetric capacitance, due to the ambiguities in mass determination of CNC films. Though the specific surface area of the convex CNC is 1.25 times higher than that of the concave CNC, the convex CNC device shows 1.7 times higher capacitance than a concave CNC device because of its more open surface morphology and electrochemically active sites formed on the surface of AAO templates²² as described above. For the branched convex type supercapacitor device, where electrochemically active surface is maximized, measured specific capacity is 3–5 times higher than regular CNC capacitor devices and 6 times higher than what has been reported for a single-layered graphene device¹⁸. Also the volumetric capacitance of the branched convex type supercapacitor (0.33 F/cm³) is only 1.36 times smaller while providing high transparency than what has been reported for laser-scribed graphene electrochemical capacitors using the same electrolyte²⁰. From the voltage versus time profile, we are able to calculate the coulombic efficiency, η using a ratio of the times for galvanostatic discharging and charging. An ideal capacitor gives 100% efficiency and has mirror inverse V shape from the galvanostatic CD curve. The coulombic efficiency for the CNC supercapacitor is 86%.

The temperature effects on capacitance and charge-discharge behaviors in CNC devices are also explored. As shown in Fig. 3c,

about three times higher capacitance (1220 μF cm⁻²) is observed at 80 °C compared to the capacitance measured at room temperature. The increase in capacitance may be partly due to the molecular alignment of PVA-H₃PO₄ chains and the excitation of charge carriers present on the imperfect sites of the CNC electrode surface with a moderate temperature increase¹⁶.

Ragone chart of the supercapacitors. To evaluate energy storage performance of the branched CNC device, energy density is plotted versus power density (Ragone chart) as shown in Fig. 3d^{24–25}. Using the internal resistance values and capacitances, energy and peak power densities for CNC supercapacitors are calculated (see the methods section). The results are compared with different thin film energy storage devices designed for flexible electronic applications. The volumetric (this includes two CNC films and the polymer electrolyte) peak power and energy densities of the branched CNC-based supercapacitors are 19 mW/cm³ and 47 μWh/cm³ respectively. This value is similar to that of the single layer graphene-based solid state supercapacitor¹⁸ and the laser-scribed graphene electrochemical capacitors²⁰ using the same electrolyte in energy density while offering high mechanical flexibility and optical transparency. In addition, the branched CNC-based supercapacitor exhibits an increase of energy densities of up to 3.1 times higher at 80 °C and has similar value to the reduced multilayer graphene oxide¹⁸ and the hydrated graphitic oxide¹⁹ in energy density. This remarkable thin film capacitor behavior can be attributed to the well-textured nanoscale features on the electrode, the significantly increased surface area in the more complex branched CNC films, the excellent conformal filling of polymer electrolyte, and the maximized active electrochemical surface area, respectively. We also speculate that the all connected graphitic structures of CNC films facilitate the charge transfer during charge/discharge processes leading to the higher power density.

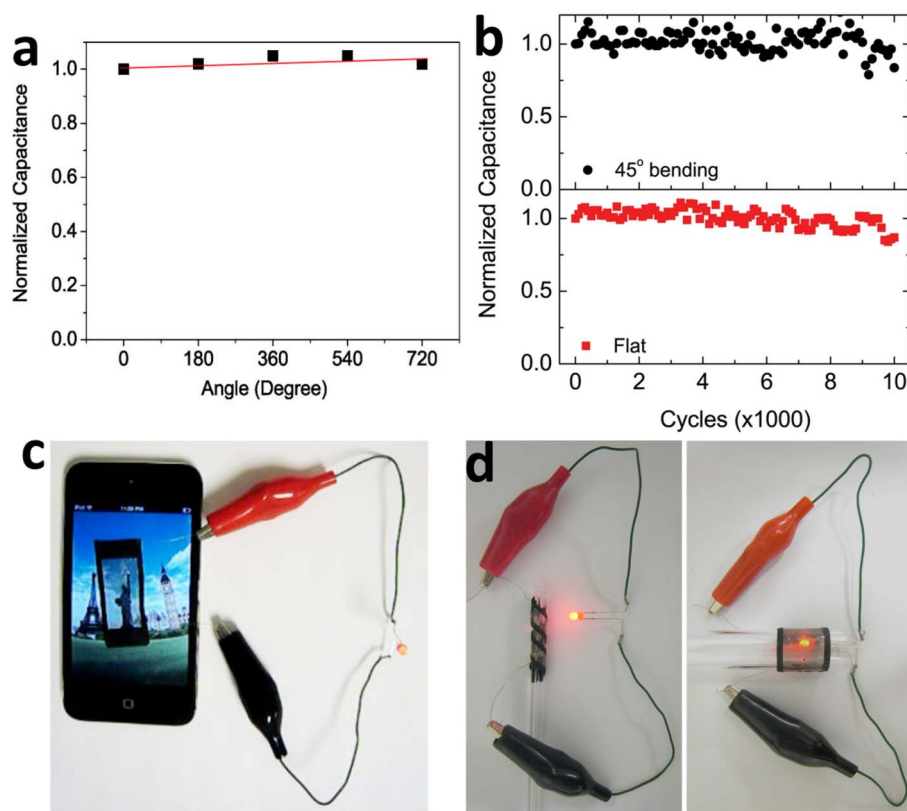


Figure 4 | Performance and demonstration of supercapacitor devices. (a) Normalized capacitance as a number of wrapping of CNC film (0 to 720°). (b) Normalized capacitance as a function of cycle-number (10,000) and w/o the mechanical deformation (45° bending). (c, d) Optical pictures demonstrating optical transparency and mechanical flexibility of a large scale CNC supercapacitor films. Note that a LED is turned on and remain stable even after helically wrapped into the differently sized glass tubes. The large area CNC supercapacitor film (3 cm by 1.5 cm) over the smartphone screen demonstrates optical transparency and the CNC capacitor films (3 cm by 1.5 cm and 3.5 cm by 0.5 cm) helically wrapped around two differently sized glass tubes (1.6 cm and 0.5 cm diameter) show excellent performance during power delivery.

Performance of the supercapacitors under mechanical deformations and their long cycle life. In order to evaluate the potential of CNC-based supercapacitors for the use as flexible energy storage, a device was placed under various mechanical deformations and its performance was analyzed. The capacitance and other electrochemical properties changes according to the number of helical wrapping of CNC capacitor film (3.5 cm by 0.5 cm) around glass tube (0.5 cm diameter) are shown in Fig. 4a and Fig. S3. CNC capacitor devices retain their superior capacitance, CV and CD properties even after helically rolled up to 720°. This excellent mechanical flexibility and integrity could be due to the effective conformal filling of polymer electrolyte into organized graphitic nanostructured film.

We also measured the long cycle life (number of charge-discharge cycles at constant current) of CNC supercapacitors w/o mechanical deformation. The normalized capacitance as a function of cycle-number is shown in the Fig. 4b. The supercapacitor devices even under mechanical stress (45° bending) show long life cycle stability: > 84% of the initial capacitance after 10,000 cycles, indicating that the performance is not limited by parasitic chemical reactions and mechanical breakdown due to swelling of the electrode or mechanical strain during charging-discharging.

Discussion

Finally the performance of our supercapacitor as flexible and transparent devices is demonstrated in Fig. 4c and 4d. For this, a prototype of a large area supercapacitor film (3 cm by 1.5 cm) was fabricated and a light-emitting diode (LED, the working potential is 1.5V) was successfully turned on for 20 min after being charged for 15 min at 2.5 V. We show that such devices could also be integrated into

unique applications where power delivery along with transparency or mechanical flexibility could be advantageous, for example as thin coatings on windows, screens, structures with different geometries etc. As a demonstration we placed our transparent supercapacitor on a smart phone screen, and during operation of the device one could clearly see the concurrent transparent nature of the devices (Fig. 4c and supplemental movie S1). In another demonstration, the devices were helically wrapped around differently sized glass tubes in high curvature yet showing excellent performance during operation (Fig. 4d and supplemental movie S2 and S3).

In summary, we demonstrated the design of transparent, flexible thin film supercapacitor devices with high performance in energy delivery. The devices were assembled using complex nano-engineered thin graphitic film electrodes with significantly increased surface area and three-dimensional structure. Unique morphological and structural features of the films enable an excellent conformal filling of polymer electrolyte and maximize active electrochemical surface area leading to high energy density. The design of the devices allows for mechanically flexible energy storage devices that could be integrated into unique applications that require high form factor and optical transparency, for example rollup displays, wearable device, and organic solar cell platforms.

Methods

Fabrications of CNC films. A CNC film with an interconnected thin graphitic texture, high specific surface area, and uniform nanopore is obtained using highly engineered AAO nanochannels as templates. Nanoporous alumina template is prepared using a standard electrochemical anodization process^{21–22,26}. Three differently engineered CNCs, which have concave, convex, and branched convex shapes, are made for the supercapacitor electrodes. For concave and convex



nanocups, a two-step anodization process is performed at 45 V in 3% oxalic acid ($C_2H_2O_2$) solution for 20 seconds to fabricate short nanochannels. Then, AAO templates are soaked in a 5% phosphoric acid solution for 1 hour at room temperature to widen nanopores. In order to produce branched convex nanocups, third anodization is carried out for 5 minutes at 25 V in 3% oxalic acid solution. Low aspect-ratio CNCs are synthesized by using a chemical vapor deposition (CVD) process at 630 °C using 10% acetylene gas as a carbon source. Then convex type nanocups are transferred to PDMS and released by dissolving AAO templates in 3.4 g copper chloride and 100 mL hydrochloric acid mixture solution with 100 mL deionized water to produce transparent and flexible graphitic carbon electrodes. For concave type nanocup devices, first the gel electrolyte is placed between two CNC with AAO templates followed by dissolving the templates. Then both sides of the film are coated by PDMS in order to facilitate the handling.

Specific surface area and mass of CNCs. The calculations are based on the following hypotheses. (1) Surface area of cap of a nanocup is consistent with that of mouth of a nanocup pore and curvature of the cap is ignored, and thus both the hexagonal cell and cylinder area in a nanocup geometry are involved into the calculation of the mass, (2) only the surface of carbon layer exposed to the electrolyte is taken into account for specific surface area, (3) the length of the C-C bonds in the curved graphene sheets is the same as in the planar sheet ($d_{c-c} = 0.1421$ nm), (4) the nanocups are composed of concentric shells and the inter-shell distance is $d_{s-s} = 0.34$ nm, (5) the total carbon layers are about 30 walls in 10 nm thickness, (6) the inter-pore distance is about 105 nm and the total nanocups in 1×1 cm² geometrical area are 1×10^{10} , (7) the specific surface area of one side of a graphene sheet is 1315 m²/g²⁷.

The surface of a carbon layer exposed to the electrolyte is: $S_c = \pi L d_e + S_{hc}$

The surface of the entire graphene sheet in one nanocup geometry is:

$$S_c = \pi L \left[nd - 2d_{s-s} \sum_{i=1}^{n-1} i \right] + nS_{hc}$$

The total mass of one nanocup geometry is: $W_c = S_c / 1315$

and thus the specific surface area of one nanocup geometry is: $SSA_{CNC} = S_c / W_c$ where L is length of nanocup, d is diameter, d_e means inner diameter for concave type and outer diameter for convex type nanocup, S_{hc} is surface of the hexagonal cell, and n is the number of graphene shells.

The calculated SSA is 39, 49 and 63 m²/g for nanocups of the concave, convex and branched convex type, respectively. The fact that each shell addition does not produce a strong increase of the surface area of the CNCs is due to the much larger increase of its mass. However, the surface of a carbon layer exposed to the electrolyte for branched CNCs is 2.9 times and 2.3 times larger than that for concave and convex CNCs.

Fabrications of CNC-based supercapacitors. The gel electrolyte is prepared by mixing PVA powder with water (1 g of PVA/ 10 mL of H₂O) and concentrated H₃PO₄ (0.8 g). PVA acts as a host for ionic conduction. The ion source comes from H₃PO₄ acid as proton donor materials. The gel electrolyte is placed between two CNC electrodes. Upon evaporation of water, the electrolyte solidifies. The polymer electrolyte shows very stable performance in the operating range of 1 V in the CNC-based supercapacitors since the voltage range of water used is closer to an aqueous electrolyte.

Characterizations of transparent and flexible supercapacitor devices.

Electrochemical properties of CNCs-based supercapacitors are analyzed using cyclic voltammetry (CV), galvanostatic charge-discharge (CD) and cyclic stability. The CV curves of CNC-based devices are measured between 0 and 1 V with various scan rates in the range of 10–500 mVs⁻¹. CV curves display nearly rectangular shape even at very high scan rates. The CD curves are obtained at a constant current density of 4.2 μAcm^{-2} for the concave CNCs and 5 μAcm^{-2} for convex CNCs and the branched convex CNCs. The capacitance and internal resistance values are determined from the slope and the initial voltage drop of the galvanostatic CD curves, respectively. The capacitances C are calculated from the galvanostatic discharge curves using $C = i / -[\Delta V / \Delta t] A = i / -\text{slope} \times A$, where C is the capacitance, i is the discharge current, the slope is the slope of the discharge curve after the iR drop, and A is the geometrical area of CNCs on the electrode. The cyclic stability is obtained by performing charge-discharge of the flat and bent CNC supercapacitor over 10,000 cycles. It is apparent that the materials retain good stability over large number of charging-discharging cycles. The efficiency (η), the power density (P) and energy density (E) of the CNC-based supercapacitors are calculated using $\eta = (t_{\text{discharging}} / t_{\text{charging}}) \times 100$, $P = V^2 / [4RV_{\text{vol}}]$ and $E = 0.5CV_{\text{vol}}^2$, respectively where $t_{\text{discharging}}$ is the discharging time, t_{charging} is the charging time, V_{vol} is the volume including area and thickness of two CNC films and a polymer electrolyte, C is the measured device capacitance, and R is the internal resistance, respectively.

- Xia, J., Chen, F., Li, J. & Tao, N. Measurement of the quantum capacitance of graphene. *Nature Nanotech.* **4**, 505–509 (2009).
- Simon, P. & Gogotsi, Y. Materials for electrochemical capacitors. *Nature Mater.* **7**, 845–854 (2008).
- Levi, M. D., Salitra, G., Levy, N., Aurbach, D. & Maier, J. Application of a quartz-crystal microbalance to measure ionic fluxes in microporous carbons for energy storage. *Nature Mater.* **8**, 872–875 (2009).

- Futaba, D. N. *et al.* Shape-engineerable and highly densely packed single-walled carbon nanotubes and their application as super-capacitor electrodes. *Nature Mater.* **5**, 987–994 (2006).
- Miller, J. R., Outlaw, R. A. & Holloway, B. C. Graphene double-layer capacitor with ac line-filtering performance. *Science* **329**, 1637–1639 (2010).
- Zhu, Y. *et al.* Carbon-based supercapacitors produced by activation of graphene. *Science* **332**, 1537–1541 (2011).
- Chmiola, J., Largeot, C., Taberna, P. L., Simon, P. & Gogotsi, Y. Monolithic carbide-derived carbon films for micro-supercapacitors. *Science* **328**, 480–483 (2010).
- Pandolfo, A. G. & Hollenkamp, A. F. Carbon properties and their role in supercapacitors. *J. Power Sources* **157**, 11–27 (2006).
- Zhang, L. L. & Zhao, X. S. Carbon-based materials as supercapacitor electrodes. *Chem. Soc. Rev.* **38**, 2520–2531 (2009).
- Izadi-Najafabadi, A. *et al.* High-power supercapacitor electrodes form single-walled carbon nanohorn/nanotube composite. *ACS Nano* **5**, 811–819 (2011).
- Kaempgen, M., Chan, C. K., Ma, J., Cui, Y. & Gruner, G. Printable thin film supercapacitors using single-walled carbon nanotubes. *Nano Lett.* **9**, 1872–1876 (2009).
- Wang, Y. *et al.* Supercapacitor devices based on graphene materials. *J. Phys. Chem. C* **113**, 13103–13107 (2009).
- Biswas, S. & Drazal, L. T. Multilayered nanoarchitecture of graphene nanosheets and polypyrrole nanowires for high performance supercapacitor electrodes. *Chem. Mater.* **22**, 5667–5671 (2010).
- Liu, C., Yu, Z., Neff, D., Zhamu, A. & Jang, B. Z. Graphene-based supercapacitor with an ultrahigh energy density. *Nano Lett.* **10**, 4863–4868 (2010).
- Stoller, M. D., Park, S. J., Zhu, Y. W., An, J. H. & Ruoff, R. S. Graphene-based ultracapacitors. *Nano Lett.* **8**, 3498–3502 (2008).
- Frackowiak, E. Carbon materials for supercapacitor application. *Phys. Chem. Chem. Phys.* **9**, 1774–1785 (2007).
- Pech, D. *et al.* Ultrahigh-power micrometer-sized supercapacitors based on onion-like carbon. *Nature Nanotech.* **5**, 651–654 (2010).
- Yoo, J. J. *et al.* Ultrathin planar graphene supercapacitors. *Nano Lett.* **11**, 1423–1427 (2011).
- Gao, W. *et al.* Direct laser writing of micro-supercapacitors on hydrated graphite oxide films. *Nature Nanotech.* **6**, 496–500 (2011).
- El-kady, M. F., Strong, V., Dubin, S. & Kaner, R. B. Laser scribing of high-performance and flexible graphene-based electrochemical capacitors. *Science* **335**, 1326–1330 (2012).
- Meng, G. *et al.* A general synthetic approach to interconnected nanowire/nanotube and nanotube/nanowire/nanotube heterojunctions with branched topology. *Angew. Chem. Int. Ed.* **48**, 1–6 (2009).
- Kang, D. W. & Suh, J. S. Fabrication temperature effect of the field emission from closed and open tip carbon nanotube arrays fabricated on anodic aluminum oxide films. *J. Appl. Phys.* **96**, 5234–5238 (2004).
- Izadi-Najafabadi, A. *et al.* Extracting the full potential of single-walled carbon nanotubes as durable supercapacitor electrodes operable at 4 V with high power and energy density. *Adv. Energy Mater.* **22**, E235–241 (2010).
- Ragone, D. V. Review of battery systems for electrically powered vehicles. *Mid-year meeting of the society of automotive engineers*, Detroit, MI, May 20–24 (1968).
- Webster, J. G. *Wiley Encyclopedia of Electrical and Electronics Engineering* vol. III. Wiley, New York (1999).
- Chun, H. K. *et al.* Engineering low-aspect ratio carbon nanostructure: nanocups, nanorings, and nanocontainers. *ACS nano* **3**, 1274–1278 (2009).
- Peigney, A., Laurent, Ch., Flahaut, E., Bacsa, R. R. & Rousset, A. Specific surface area of carbon nanotubes and bundle of carbon nanotubes. *Carbon* **39**, 507–514 (2001).

Acknowledgment

The authors acknowledge the financial support from Fundamental R&D Program for Core Technology of Materials in the Ministry of Knowledge Economy, Republic of Korea, and National Science Foundation-CMMI grant (0927088). MGH and PMA acknowledge financial support from US Army Research Laboratory/Army Research Office (No. W911NF) and Exotic Nanocarbons, Japan Regional Innovation Strategy Program by the Excellence, JST.

Author contributions

H.Y.J., P.M.A., and Y.J.J. designed experiments and H.Y.J. carried out most experiments. M.B.K. fabricated the carbon nanocups and M.G.H. designed schematics. H.Y.J. wrote the manuscript, and all authors discussed the results and contributed to revisions.

Additional information

Supplementary information accompanies this paper at <http://www.nature.com/scientificreports>

Competing financial interests: The authors declare no competing financial interests.

License: This work is licensed under a Creative Commons

Attribution-NonCommercial-NoDerivative Works 3.0 Unported License. To view a copy of this license, visit <http://creativecommons.org/licenses/by-nc-nd/3.0/>

How to cite this article: Jung, H.Y., Karimi, M.B., Hahm, M.G., Ajayan, P.M. & Jung, Y.J. Transparent, flexible supercapacitors from nano-engineered carbon films. *Sci. Rep.* **2**, 773; DOI:10.1038/srep00773 (2012).